# Definition of Simplified Frequency-Domain Volterra Models With Quasi-Sinusoidal Input

Marco Faifer, *Senior Member, IEEE*, Christian Laurano, *Student Member, IEEE*, Roberto Ottoboni, *Fellow, IEEE*, Marco Prioli, Sergio Toscani[ID], *Member, IEEE*, and Michele Zanoni, *Student Member, IEEE*

*Abstract*— The Volterra approach to the modeling of nonlinear systems has been employed for a long time thanks to its conceptual simplicity and flexibility. Its main drawback lies in the number of coefficients, which rapidly grows with memory length and nonlinearity order. In some important cases, such as power system applications, the input signal is periodic and contains a fundamental component that is much larger with respect to the others. This peculiarity can be exploited in order to dramatically reduce the number of coefficients defining the frequency-domain Volterra model with slight drawbacks in terms of accuracy. A systematic procedure for the definition of simplified, frequency-domain models of arbitrary order is proposed. Thanks to the simplification, very high orders of nonlinearity can be managed. The proposed approach has been employed to model the behavior of two electrical devices with different amount of nonlinearity, and that of a power grid containing linear and nonlinear loads. Accuracy is discussed and compared with that obtained with a conventional Volterra model defined by a similar number of coefficients. Results show the effectiveness of the approach, which is particularly suitable to model and test voltage and current transducers as well as other ac power system devices.

*Index Terms*— Nonlinear systems, power quality, Volterra series, transducer, system identification.

## I. INTRODUCTION

All physical systems exhibit a certain degree of nonlinearity. However, in many cases, nonlinear systems are modeled by using the conventional, well-known linear time invariant (LTI) approach, thus avoiding the inherent complication of nonlinear modeling [1]–[4]. This is possible only when the impact of the nonlinearities on the output is small with respect to the target accuracy, thanks to the limited range of the input signal or to the weakly nonlinear behavior of the system. When this condition is not met, models able to take into account also nonlinear effects are required. Since the complexity of the phenomena to be studied as well as the accuracy requirements are continuously growing in the last years, nonlinear modeling is becoming more and more important.

Nonlinear modeling is somewhat a hard topic, especially when there is lack of knowledge about the structure and the operating principle of the device to be represented. In this case, a black-box, nonparametric model has to be adopted [5]. A broad variety of techniques based on very different approaches can be found in the literature [6]. Among them, the Volterra approach to the modeling of nonlinear time invari-ant (NTI) systems [7], [8] has been employed for a long time, and it is still widely employed in many applications [9]–[13].

The main advantage lies in its conceptual simplicity, since it represents a blend between the usual LTI system theory (both in time and frequency domain) and the Taylor series expansion. For this reason, models based on the truncated Volterra series are often called polynomial models [14]. The main drawback is that a (discrete) Volterra model is defined by a number coefficients that grows more than exponentially with the considered order of nonlinearity [14]. For this reason, only very low orders of nonlinearity (usually second and third) are employed in most practical applications [9], [10]–[13]: otherwise, the computational burden and the identification pro-cedure become troublesome. Similarly to a low-order Taylor expansion, such polynomial models may be not accurate for a broad input range, and in any case they are not the proper tools to represent strong nonlinearities. For this reason, several techniques able to simplify (or "to prune") Volterra models have been studied and proposed in the literature [15]–[21]. Most of these methods are specifically devoted to the behav-ioral modeling of radio frequency power amplifiers and, in general, to communication system application. The time-domain formulation of truncated Volterra systems is con-sidered, and kernels are pruned assuming a "near-diagonal" structure, exploiting some a priori knowledge or using matching pursuit techniques.

However, sometimes the target is predicting the steady-state response of a system to a periodic input containing a fairly low number of spectral components: a frequency-domain Volterra approach is usually much more effective [8], [14],[22], [23]. Albeit it is not as widely employed as the cor-responding time-domain counterpart, in this case it often allows a considerable reduction in the number of coefficients. Furthermore, in some important applications, such as in ac power systems, the input (voltage or current) contains a fundamental spectral component that is much larger than its harmonics. This characteristic of the input signal can be exploited to drastically reduce the number of coefficients, thus enabling the employment of frequency-domain Volterra models of unprecedented order. The approach has been applied in [24] to a fifth order polynomial system.

In this paper, a systematic procedure to define and identify simplified frequency-domain polynomial models having an arbitrary order of nonlinearity is presented.

Manuscript received March 28, 2017;
revised August 3, 2017, September 5, 2017, and September 29, 2017;
accepted September 29, 2017.
Date of publication November 1, 2017;
date of current version April 2, 2018.

This paper was recommended by Associate Editor E. Blokhina.(Corresponding author: *Sergio Toscani.*)
M. Faifer, C. Laurano, R. Ottoboni, S. Toscani, and M. Zanoni are with the Dipartimento di Elettronica, Informazione e Bioingegneria, Politecnico di Milano, 20133 Milano, Italy (e-mail: sergio.toscani@polimi.it).
M. Prioli is with CERN, CH-1211 Geneva, Switzerland.
Color versions of one or more of the figures in this paper are available online at http://ieeexplore.ieee.org.

The proposed technique is particularly suited to obtain a behavioral representation of power system components, when a physically-based model is not available, difficult to be identified, or not accurate enough. As case studies, the technique is applied to model two power system devices, having a different level of nonlinearity: a saturable inductor and a voltage transformer. Furthermore, the approach is applied to represent the current-voltage relationship of a simple grid made up of the connection of both linear and nonlinear loads. Simplified models up to the eleventh order are employed. Obtained accuracy is discussed and compared with that achieved with a well-known reference method, namely a full frequency-domain Volterra model described by a similar number of coefficients.

## II. The Volterra Representation of NTI Systems

### A. Time-Domain Volterra Models

Let us consider a NTI, single input-single output system; its generic Volterra-series representation is given by the following expression

$$y\left(t\right) = h^0 + \sum_{i=1}^{\infty} y^i\left(t\right) \tag{1}$$

$h^0$ is a constant that represents the system output $y$ when the input is identically zero; without loss of generality, the case $h^0 = 0$ will be considered in the following. Under this assumption, the output $y$ can be decomposed into the sum of an infinite number of terms $y^i$, each representing the contribution of a so-called $i$-th order homogeneous subsystem. In turn, the output of the subsystem is obtained as the $i$-fold convolution between a function $h^i$ of $i$ variables and the input $x$:

$$y^i\left(t\right) = \int_{-\infty}^{+\infty} \cdots \int_{-\infty}^{+\infty} h^i\left(\tau_1, .., \tau_i\right) \prod_{p=1}^{i} x\left(t - \tau_p\right) d\tau_p \tag{2}$$

The time-domain behavior of the $i$-th order subsystem is defined by $h^i$ which is called $i$-th order kernel. The similarity of (2) with respect to the convolution representation of linear systems is evident; in particular, it can be noticed that the first order subsystem is LTI. For this reason, $h^i$ is also known as the generalized impulse response of the $i$-th order subsystem. Physical systems are causal: this implies that the generalized impulse responses must be zero when at least an argument is negative. Therefore, the lower integration limits appearing in (2) can be set to zero.

The number of kernels defining a Volterra model is infinite, hence a practical implementation is not feasible. For this reason, the maximum order $I$ of the homogenous subsystems has to be finite, like when a $C^{\infty}$ function is approximated by its truncated Taylor expansion. The sum appearing in (1) has to be upper bounded to $I$, so that an $I$-th order Volterra (or polynomial) system is obtained.

Polynomial models are typically implemented as discrete-time systems by means of digital signal processing techniques. Input and output are assumed to be properly sampled signals (thus avoiding aliasing artifacts) therefore the kernels become functions of discrete variables. The multiple integrations in (2) reduce in cascaded summations containing infinite terms. Being it not possible from a practical point of view, summation indexes are limited to a finite number of samples $K$-1, which is called memory length. This corresponds to the assumption that the amplitudes of the generalized impulse responses become negligible after $K$ samples. Following these considerations, the generic expression of a causal, discrete-time $I$-th order Volterra system with finite memory length becomes:

$$\begin{aligned} y\left(n\right) &= \sum_{i=1}^{I} y^i\left(n\right) \\ y^i\left(n\right) &= \sum_{k_1=0}^{K-1} \cdots \sum_{k_i=0}^{K-1} h^i\left(k_1, \ldots, k_i\right) \prod_{p=1}^{i} x\left(n - k_p\right) \end{aligned} \tag{3}$$

The kernel $h^i$ belonging to the $i$-th order homogeneous subsystem is a function having $i$ arguments, each of them assuming a finite number $K$ of values. Therefore, $h^i$ can be represented as an $i$-dimensional matrix, thus consisting of $K^i$ coefficients. The behavior of the whole system is characterized by a number $c_{TD}$ of coefficients:

$$c_{TD} = \sum_{i=1}^{I} K^i \tag{4}$$

It can be noticed that when the arguments of $h^i$ in (3) are permuted, the quantity to be multiplied, which is the product between different samples of the input signal, remains the same. This means that the same input-output relationship of the Volterra model can be obtained with infinite sets of kernels, because not all of the coefficients are independent. It is possible to show that $c_{TD,ind}$, namely the number of independent coefficients of an $I$-th order Volterra system having a memory length of $K$ samples, is [14]:

$$c_{TD,ind} = \sum_{i=1}^{I} \frac{(K + i - 1)!}{(K - 1)!i!} \tag{5}$$

In order to remove this dependency, the generic $i$-th order kernel $h^i$ can be replaced with its symmetric representation $h^i_{sym}$, which is invariant with respect to the permutation of the arguments. The symmetric form implicitly contains constraints between the coefficients, so that a one-to-one correspondence between input/output relationship of an $i$-th order homogeneous system and its symmetric kernel is established. In any case, it should be noted the number of independent coefficients rapidly grows with $I$ and $K$, thus preventing the employment of high-order Volterra systems.

### B. Frequency-Domain Volterra Models

In some applications it is interesting to predict the steady-state response to a periodic excitation, characterized by the fundamental angular frequency $\omega_0$ and the maximum harmonic order $N_X$, so that the two-sided input spectrum consists of $M = 2N_X+1$ (complex) components. In this case a frequency-domain approach is generally preferred, since the output can be computed starting from a partial knowledge of the model. For example, under the LTI assumption, only its frequency response function evaluated at the input harmonics is required. The things are obviously trickier when an $I$-th order Volterra model is considered. Having assumed that both the input and output signals are properly sampled (thus supposing negligible aliasing and spectral leakage), the discrete Fourier transform can be applied to (3), which allows obtaining the frequency-domain representation of the Volterra system. Considering the symmetrical form of the kernels, the following relation between the input spectrum $X(jn\omega_0)$ and output spectrum $Y(jm\omega_0)$ is derived:

$$Y(m) = \sum_{i=1}^{I} Y^i(m)$$

$$Y^i(m) = \sum_{-N \leq n_1,\ldots,n_i \leq N} H^i(n_1,\ldots,n_i) \prod_{p=1}^{i} X(n_p) \quad (6)$$

Subject to:

$$\sum_{p=1}^{i} n_p = m \quad (7)$$

For the sake of brevity, the input and output spectra $X(jn\omega_0)$ and $Y(jm\omega_0)$ are indicated as $X(n)$ and $Y(m)$, where $n$ and $m$ denotes the generic harmonic orders of the input and output spectral components respectively. From (6), the $m$-th output harmonic is due to the sum of different contributions, each produced by a homogeneous subsystem. In turn, the contribution of the $i$-th order subsystem results from the products between $i$ spectral components of the input subject to (7) (hence the sum of their harmonic orders is equal to $m$) weighted by $H^i$. The latter can be represented as an $i$-dimensional matrix that associates a complex number to a set of $i$ spectral components of the input signal. It is obtained by applying a multivariate discrete Fourier transform to the generalized impulse response $h^i$. Because of the evident analogy with the frequency domain representation of LTI systems, $H^i$ is often denoted as $i$-th order generalized frequency response function (GFRF). Since the input spectrum contains $M$ harmonics, $H^i$ consists of $M^i$ elements, but as for the time-domain representation not all of them are independent. Instead, it can be easily shown that $c_{FD,ind}$, namely the number of independent coefficients defining the frequency-domain $I$-th order polynomial system is given by (5), but substituting $K$ with $M$:

$$c_{FD,ind} = \sum_{i=1}^{I} \frac{(M+i-1)!}{(M-1)!i!} \quad (8)$$

Even in this case, it is possible to use special forms of the GFRFs, such as the symmetric representation, in order to remove the indetermination of its coefficients.

In many practical applications, $M$ is considerably smaller than $K$. This obviously happens when the number of input harmonics is fairly low, and also when the system dynamics is slow, but the spectral content of the input signal demands for a fairly high sampling rate. It should be noted that while the coefficients defining a GFRF are complex, those appearing in a generalized impulse response are real numbers. On the other hand, assuming that the system input and output are real, the circular Hermitian symmetry (called Hermitian symmetry in the following for the sake of brevity) of their spectra further reduces the number of independent coefficients [14], [22].

## III. Model Reduction With Quasi-Sinusoidal Excitation

Although the frequency-domain approach allows a consistent simplification in modeling the steady-state response of a Volterra system to periodic inputs, the number of coefficients rapidly grows with the number $N$ of input harmonics and nonlinearity order $I$. However, it is possible to exploit a peculiarity of the input signal in order to achieve a consistent reduction in the number of coefficients. In some important cases, such as the modeling of ac power system devices, the (real) input signal contains a main, fundamental component that is much greater than its harmonics. As explained in the previous section, the output spectrum results from $I$ homogeneous subsystems; the contribution of the $i$-th order subsystem is a weighted sum of $i$-th order intermodulation products, where the weights are given by the corresponding GFRF. Because of the spectral power distribution of the input signal, the highest $i$-th order intermodulation products are those containing solely the fundamental component, while the lowest ones are those involving only harmonics. In [24] it has been proposed to simplify the frequency-domain Volterra model by neglecting the contributions to the output due to intermodulation products containing more than a harmonic. The class of input signals such that this approximation leads to results complying with the target accuracy is defined as *quasi sinusoidal*. The proposed approach was applied to a $5^{\text{th}}$ order Volterra system, but a systematic procedure to implement the method for a generic order of nonlinearity and number of input harmonics, which is target of this paper, was not developed.

### A. Generalized Frequency Response Functions Under Quasi-Sinusoidal Conditions

Let us consider an $I$-th order polynomial system satisfying the quasi-sinusoidal assumption. Let us suppose that the input signal $x$ is real, periodic and characterized by the fundamental angular frequency $\omega_0$. In order to define the simplified, $i$-th order GFRF it is easier to start from the spectrum of the output signal $y$, thus identifying all the intermodulation products that may contribute to the $m$-th harmonic component $Y(m)$, where:

$$0 \leq m \leq N_Y \quad (9)$$

On the one hand, being $y$ real, it is possible to consider just the right part of its spectrum. On the other hand, it is useful to employ the two-sided representation of the input signal spectrum. In this case, the terms having the highest amplitude are $X(1)$ as well as its conjugate $X(-1)$, because of the quasi-sinusoidal assumption. While studying the contribution of the $i$-th order subsystem, the fundamental (or its complex conjugate) appears at least $i-1$ times in a generic intermodulation product $W^i$, which therefore can be written as:

$$W^i\left(i_p, i_m, n\right) = X(1)^{i_p}\, X(-1)^{i_m}\, X(n) \tag{10}$$

Subject to the condition:

$$i_p + i_m + 1 = i \tag{11}$$

Considering the symmetrical form of the GFRF, the contribution of the $i$-th order subsystem to the $m$-th output harmonic results:

$$Y^i(m) = \sum_{-N\le n\le N} H^i_{sym}\left(i_p, i_m, n\right) W^i\left(i_p, i_m, n\right) \tag{12}$$

Having introduced:

$$H^i_{sym}\left(i_p, i_m, n\right) = H^i_{sym}\left(\underbrace{1,\ldots,1}_{i_p}, \underbrace{-1,\ldots,-1}_{i_m}, n\right) \tag{13}$$

According to (7), the output harmonic order and the components appearing in the intermodulation product must satisfy the constraint:

$$i_p - i_m + n = m \tag{14}$$

From these considerations, the $i$-th order GFRF coefficients contributing to the $m$-th output harmonic are those identified by $i_p$, $i_m$, $n$ satisfying the constraints:

$$\begin{cases} i_m = i - 1 - i_p \\ n = m - i_p + i_m \\ 0 \le i_p \le i-1 \end{cases} \tag{15}$$

It can be noticed that the number of coefficients for each output harmonic and order of nonlinearity is equal to $i$. Therefore, (12) can be written in vector form as:

$$Y^i(m) = \mathbf{W}^{iT}_m \mathbf{H}^i_m \tag{16}$$

$\mathbf{W}^i_m$ and $\mathbf{H}^i_m$ are $i \times 1$ vectors containing respectively the intermodulation products and the coefficients of the $i$-th order subsystem affecting the $m$-th output harmonic. In turn, the output of the $I$-th order polynomial system is:

$$Y(m) = \mathbf{W}^T_m \mathbf{H}_m = \begin{bmatrix} \mathbf{W}^1_m \\ \mathbf{W}^2_m \\ \vdots \\ \mathbf{W}^{I-1}_m \\ \mathbf{W}^I_m \end{bmatrix}^T \begin{bmatrix} \mathbf{H}^1_m \\ \mathbf{H}^2_m \\ \vdots \\ \mathbf{H}^{I-1}_m \\ \mathbf{H}^I_m \end{bmatrix} \tag{17}$$

Where $\mathbf{W}_m$ and $\mathbf{H}_m$ are column vectors whose length is:

$$L = \sum_{i=1}^{I} i = \frac{I(I+1)}{2} \tag{18}$$

Since the output spectrum is characterized by $N_Y + 1$ independent components, the overall number of coefficients defining the $I$-th order polynomial system is:

$$c_{QS} = (N_Y + 1)\frac{I(I+1)}{2} \tag{19}$$

*B. Removal of Redundancies*

The reduction in the number of coefficients with respect to the complete Volterra model is evident when (19) is compared with (8): now it is approximately proportional to the square of the nonlinearity order. However, some of the $c_{QS}$ coefficients under quasi sinusoidal conditions are redundant. Dependencies result from the selected problem formulation, expressed by (13). While it allows an easy, automated implementation, its drawback is that the same intermodulation product is indexed by two different sets of $i_p$, $i_m$ and $n$. In fact, for each $i_p$ and $i_m$ subject to (11), it follows:

$$W^i\left(i_p, i_m, 1\right) = W^i\left(i'_p, i'_m, -1\right)$$
$$\Leftrightarrow \exists\ \ 0 \le i'_p, i'_m \le i-1 : \begin{cases} i'_p = 1 + i_p \\ i'_m = 1 - i_m \end{cases} \tag{20}$$

Redundancies have to be searched in the same vector $\mathbf{W}^i_m$ since duplicated intermodulation products necessarily affect the same output harmonic. $\mathbf{W}^i_m$ can be written as:

$$\mathbf{W}^i_m = \begin{bmatrix} W^i(i-1, 0, -i+m+1) \\ W^i(i-2, 1, -i+m+3) \\ \vdots \\ W^i(1, i-2, i+m-3) \\ W^i(0, i-1, i+m-1) \end{bmatrix} \tag{21}$$

The $k$-th element of this vector can be written as:

$$\mathbf{W}^i_m(k) = W^i(i-k, k-1, -i+m-1+2k) \qquad 1 \le k \le i \tag{22}$$

$\mathbf{W}^i_m$ contains no more than a duplicated element; in fact, there is at best only an integer $k^i_m$ solving:

$$-i + m - 1 + 2k^i_m = -1 \qquad 1 \le k^i_m \le i \tag{23}$$

It results:

$$i \ge 2 + m \qquad k^i_m = \frac{i-m}{2} \tag{24}$$

Therefore, from (24), a redundancy may be present in $\mathbf{W}^i_m$ only if both $i$ and $m$ are even or odd. $k^i_m$, if exists, represents the index of the duplicated element to be removed from $\mathbf{W}^i_m$. It is useful to graphically represent the vectors $\mathbf{W}^i_m$ containing redundancies, as shown in Fig. 1, which also reports the indexes of the elements to be deleted.

While considering the $i$-th order subsystem, the number of redundant coefficients is equal to the number of red squares appearing in the $i$-th row of Fig. 1. It is easy to notice that said number corresponds to the integer part of $i/2$. Therefore, by using a well-known expression, the overall number of duplicated intermodulation products $c_d$ to be omitted from the whole model results:

$$c_d = \sum_{i=1}^{I}\left\lfloor \frac{i}{2} \right\rfloor = \left\lfloor \frac{I^2}{4} \right\rfloor \tag{25}$$

where $\lfloor\cdot\rfloor$ denotes the integer part.

| $\mathbf{W}_m^i$ | **Output Harmonic Order *m*** | | | | | | | | | | |
|---|---|---|---|---|---|---|---|---|---|---|---|
| **Nonlinearity Order *i*** | **0** | **1** | **2** | **3** | **4** | **5** | **6** | **7** | **8** | **9** | $\cdots$ |
| **1** | | | | | | | | | | | $\cdots$ |
| **2** | 1 | | | | | | | | | | $\cdots$ |
| **3** | | 1 | | | | | | | | | $\cdots$ |
| **4** | 2 | | 1 | | | | | | | | $\cdots$ |
| **5** | | 2 | | 1 | | | | | | | $\cdots$ |
| **6** | 3 | | 2 | | 1 | | | | | | $\cdots$ |
| **7** | | 3 | | 2 | | 1 | | | | | $\cdots$ |
| **8** | 4 | | 3 | | 2 | | 1 | | | | $\cdots$ |
| **9** | | 4 | | 3 | | 2 | | 1 | | | $\cdots$ |
| **10** | 5 | | 4 | | 3 | | 2 | | 1 | | $\cdots$ |
| **11** | | 5 | | 4 | | 3 | | 2 | | 1 | $\cdots$ |
| $\vdots$ | $\vdots$ | $\vdots$ | $\vdots$ | $\vdots$ | $\vdots$ | $\vdots$ | $\vdots$ | $\vdots$ | $\vdots$ | $\vdots$ | $\ddots$ |

Fig. 1. Redundant intermodulation products to be removed from $\mathbf{W}_m^i$. Numbers in the red squares are their indexes $k_m^i$.

Unfortunately, the model contains other redundant coefficients. The reason is that the constraint about the real-valued output signal has not been fully imposed. Only the right (positive) part of the spectra has been considered as in (9), which corresponds to impose that the ac part of the output signal has to be real-valued. However, also the dc component at the output must be real-valued. Let us consider the generic vector $\mathbf{W}_0^i$, having removed the redundant element in position $k_0^i = i/2$ when $i$ is even, as pointed out by Fig. 1; following (21) this vector can be written as:

$$\mathbf{W}_0^i = \begin{bmatrix} W^i\left(i-1,0,-i+1\right) \\ W^i\left(i-2,1,-i+3\right) \\ \vdots \\ W^i\left(1,i-2,i-3\right) \\ W^i\left(0,i-1,i-1\right) \end{bmatrix} = \begin{bmatrix} X\left(1\right)^{i-1} X\left(-1\right)^{0} X\left(-i+1\right) \\ X\left(1\right)^{i-2} X\left(-1\right)^{1} X\left(-i+3\right) \\ \vdots \\ X\left(1\right)^{1} X\left(-1\right)^{i-2} X\left(i-3\right) \\ X\left(1\right)^{0} X\left(-1\right)^{i-1} X\left(i-1\right) \end{bmatrix} \quad (26)$$

Having removed the redundancies, the total number of elements in $\mathbf{W}_0^i$ is always odd. Let us introduce the index $k_c^i$ of the middle element:

$$k_c^i = \left\lfloor \frac{i+1}{2} \right\rfloor \quad (27)$$

Since the input signal is real, its spectrum is Hermitian; therefore, from (26) it can be easily checked that the vectors $\mathbf{W}_0^i$ are Hermitian. The dc output component has to be real; considering (16) with $m$ =0 implies that also $\mathbf{H}_0^i$ have to be Hermitian. From these considerations, it follows:

$$\begin{aligned} Y^i(0) &= \mathbf{W}_0^{iT}\mathbf{H}_0^i \\ &= 2\Re\left[\sum_{k=1}^{k_c^i-1} \mathbf{W}_0^i(k)\,\mathbf{H}_0^i(k)\right] + \mathbf{W}_0^i\left(k_c^i\right)\mathbf{H}_0^i\left(k_c^i\right) \end{aligned} \quad (28)$$

Hence, considering just the first $k_c^i$ elements of $\mathbf{H}_0^i$ and $\mathbf{W}_0^i$, it is possible to rewrite (28) as:

$$Y^i(0) = \Re\left(\mathbf{W}_0^{iT}\mathbf{H}_0^i\right) \quad (29)$$

Considering all the contributions to the dc output component $Y(0)$:

$$Y(0) = \Re\left(\mathbf{W}_0^T\mathbf{H}_0\right) = \Re\left\{\begin{bmatrix} \mathbf{W}_0^1 \\ \mathbf{W}_0^2 \\ \vdots \\ \mathbf{W}_0^{I-1} \\ \mathbf{W}_0^I \end{bmatrix}^T \begin{bmatrix} \mathbf{H}_0^1 \\ \mathbf{H}_0^2 \\ \vdots \\ \mathbf{H}_0^{I-1} \\ \mathbf{H}_0^I \end{bmatrix}\right\} \quad (30)$$

As from (28) $Y^i(0)$, which is the contribution to the DC output component related to the $i$-th order subsystem, can be written as a linear combination of $k_c^i$ intermodulation products. This means that, for the $i$-th order subsystem, $k_c^i - 1$ coefficients are redundant. The total number $c_{d,0}$ of coefficients that have to be removed from the polynomial model is:

$$c_{d,0} = \sum_{i=1}^{I}\left(k_c^i - 1\right) = \sum_{i=1}^{I}\left\lfloor \frac{i-1}{2} \right\rfloor = \left\lfloor \frac{(I-1)^2}{4} \right\rfloor \quad (31)$$

Finally, using (19), (25) and (31), the overall number of independent coefficients $c_{QS,red}$ defining the simplified Volterra model results:

$$c_{QS,red} = \left(N_Y+1\right)\frac{I\left(I+1\right)}{2} - \left\lfloor \frac{I^2}{4} \right\rfloor - \left\lfloor \frac{(I-1)^2}{4} \right\rfloor \quad (32)$$

$I$ of them are real-valued, the remaining are complex numbers.

It should be noticed that the number of coefficients defining the $I$-th order simplified Volterra model has been obtained by counting all possible intermodulation products that may contribute to an output spectral components. Therefore, in practice, the actual number of coefficients may be lower than $c_{QS,red}$. This typically happens at the highest values of $m$ because the input signal is band-limited.

## IV. Case Studies and Numerical Simulations

In the previous section, a method that allows obtaining simplified frequency-domain polynomial models having arbitrary nonlinearity order has been explained. Identifying such a model means, for each output harmonic order $m$, inverting (17) in order to compute $\mathbf{H}_m$. As discussed in [24], this is not possible by measuring the response to a single input signal (unless $I = 1$), since the problem is undetermined. Instead, the system response to a proper set of $P$ quasi-sinusoidal identification signals has to be considered. For a generic $m$-th order output harmonic, a column vector $\mathbf{Y}_{id,m}$ containing the $P$ system responses to the set of identification signals can be defined. As from (17), for each input signal a vector of intermodulation products affecting the $m$-th order output harmonic can be written. A matrix $\mathbf{W}_{id,m}$ is obtained by horizontally concatenating these vectors. Therefore, the following matrix equation is introduced:

$$\mathbf{Y}_{id,m} = \mathbf{W}_{id,m}^T\mathbf{H}_m \quad (33)$$

The vector of coefficients $\mathbf{H}_m$ can be obtained in a least square sense by using the left inverse of $\mathbf{W}_{id,m}^T$.

$$\mathbf{H}_m = \left(\mathbf{W}_{id,m}^T\right)^{\dagger}\mathbf{Y}_{id,m} \quad (34)$$

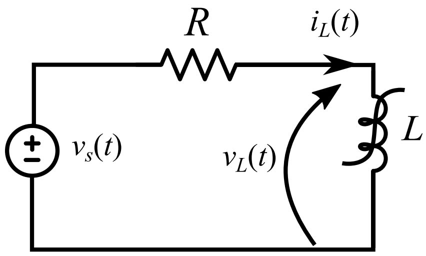


Fig. 2. Equivalent circuit of the nonlinear inductor.

TABLE I
NONLINEAR INDUCTOR PARAMETERS

| $N$ | $A$ [cm$^2$] | $l$ [mm] | $R$ [Ω] | $V_n$ [V] |
|---|---|---|---|---|
| 100 | 10 | 50 | 50 | 40 |

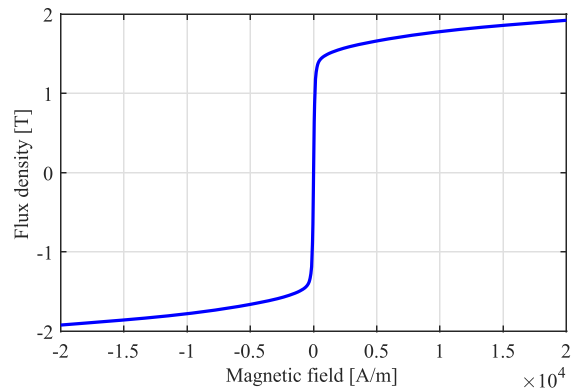


Fig. 3. Single-valued *b-h* curve of the core material.

First of all, this requires that $P$ has to be greater or equal than $L$, namely the maximum length of $\mathbf{H}_m$ obtained by (18). In addition, the spectral content of the set of identification signals has to be properly designed such that $\mathbf{W}_{id,m}^T$ has full row rank.

It is clear that uncertainties affecting input and output signal measurements may play a significant role in the model accuracy. Since the target of this paper is evaluating the intrinsic impact of the proposed simplification, the technique is applied by simulating the measurement process. For this purpose, equivalent circuits of two typical nonlinear devices that can be found in power grids, and that of a more complex electrical network have been implemented. Input and output signals have been sampled with a 10 kHz sampling rate, and the proposed simplified polynomial modeling technique has been applied to represent the behavior of these systems.

The first case study consists of modeling the voltage-current relationship of a saturable inductor, representing a typical passive, nonlinear load. The second example consists in representing the response of a voltage instrument transformer (VT) to a distorted input voltage. This device has considerably weaker nonlinearities; nevertheless a much smaller target accuracy is required in this case. The equivalent circuits of both the devices have been implemented, and their input-output relationships have been represented with simplified frequency-domain polynomial models of different orders (from 1 to 11). The target of the third example is predicting the current supplied by a distorted ac voltage generator to a grid made of three different loads: a linear load, a saturable inductor and an ideal full-bridge diode rectifier having an ohmic-inductive load connected to its dc side.

### A. Saturable Inductor

The proposed model has been applied to represent the frequency-domain relationship between the voltage $v_s$ and the current $i_L$ of an iron core inductor. The input voltage is supposed to be quasi-sinusoidal, containing a 50 Hz fundamental, harmonics up to the 7$^{\text{th}}$ order and a dc component.

The inductor has been simulated by implementing the equivalent circuit shown in Fig. 2. The parameters are listed in TABLE I, being $N$ the number of turns, $A$ the core cross-sectional area, $l$ the average length of the magnetic circuit, $R$ the winding resistance, $V_n$ the rated rms voltage (50 Hz rated frequency). The single-valued *b-h* curve of the iron core material is reported in Fig. 3; the flux linkage to current relationship is easily obtained by using the geometrical parameters.

The target is identifying simplified Volterra models of different orders $I$, ranging from 1 (linear model) to 11. For each nonlinearity order, a set of 30 $L$ quasi-sinusoidal voltage signals has been employed for computing the coefficients, so that in any case the inverse problem is heavily overdetermined.

These identification signals consist of a fundamental component whose amplitude is randomly extracted by using a uniform probability density function in the range between 60% and 120% of the rated voltage. The dc component and the harmonics have the same amplitude, corresponding to 2% of the fundamental component. The polarity of the dc term is random while the harmonic phases have been randomly obtained considering a uniform probability density function in the interval $[-\pi, \pi]$. The coefficients of the eleven simplified polynomial models have been obtained from (34).

The accuracy of the different models in predicting the generic $m$-th order harmonic of the current $I_L(m)$ for a given input voltage spectrum has been evaluated by using the total vector error with respect to the fundamental component:

$$\text{TVE}^1(m) = \frac{\left|I_L(m) - I_L^{act}(m)\right|}{\left|I_L^{act}(1)\right|} \tag{35}$$

It represents the distance on the complex plane between the predicted and the actual amplitude of the system output ($I_L(m)$ and $I_L^{act}(m)$ respectively) with respect to the amplitude of the actual fundamental output component ($I_L^{act}(1)$). $\text{TVE}^1(m)$ has been computed for every model considering each identification signal; as synthetic performance indexes, the 95$^{\text{th}}$ percentile values $\text{TVE}_{95}^1(m)$ have been obtained for each model and output harmonic; results are shown in Fig. 4 while the most significant values are summarized in TABLE II.

As expected, the employment of a linear model results in extremely high errors in predicting the output harmonics. Considering the fundamental component, $\text{TVE}_{95}^1$ is about 54%. Errors reduce dramatically by employing the proposed

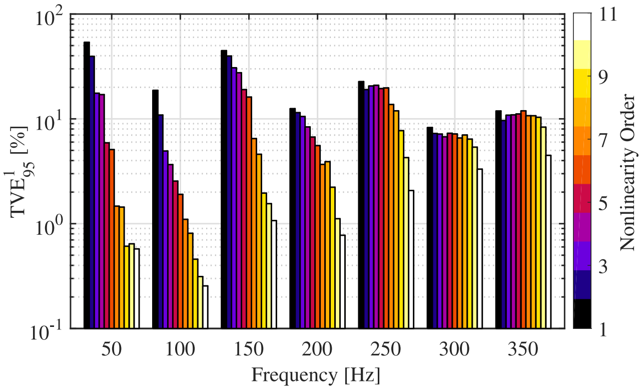


Fig. 4. Accuracy comparison between simplified polynomial models of the nonlinear inductor.

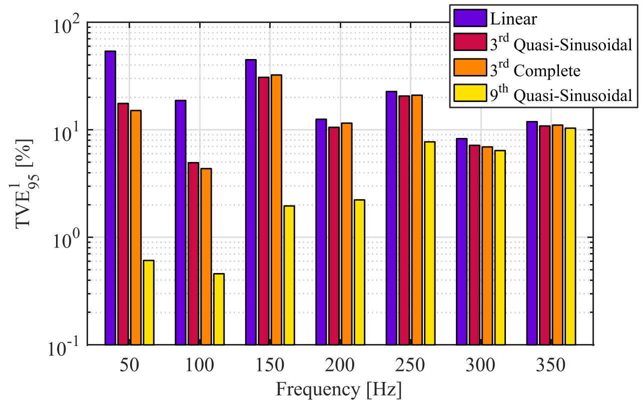


Fig. 5. Comparison between linear, complete third order, simplified third order and simplified ninth order polynomial models of the nonlinear inductor.

TABLE II

NONLINEAR INDUCTOR $\mathrm{TVE}^1_{95}$: LINEAR AND SIMPLIFIED POLYNOMIAL MODELS

| $\mathrm{TVE}^1_{95}$ [%] | Harmonic Order | | | | | | |
|---|---|---|---|---|---|---|---|
| | **1** | **2** | **3** | **4** | **5** | **6** | **7** |
| **Linear** | 53.8 | 18.7 | 44.8 | 12.5 | 22.7 | 8.3 | 11.9 |
| **QS 11th** | 0.57 | 0.26 | 1.07 | 0.77 | 2.07 | 3.31 | 4.49 |

TABLE III

INDUCTOR $\mathrm{TVE}^1_{95}$: COMPLETE AND SIMPLIFIED POLYNOMIAL MODELS

| $\mathrm{TVE}^1_{95}$ [%] | Harmonic Order | | | | | | |
|---|---|---|---|---|---|---|---|
| | **1** | **2** | **3** | **4** | **5** | **6** | **7** |
| **3rd QS** | 17.6 | 4.94 | 30.7 | 10.5 | 20.6 | 7.16 | 10.9 |
| **3rd Complete** | 15.1 | 4.35 | 32.3 | 11.5 | 21.0 | 6.93 | 11.1 |
| **9th QS** | 0.61 | 0.46 | 1.96 | 2.23 | 7.72 | 6.41 | 10.4 |

approach and increasing the order of nonlinearity. For example, the eleventh order model achieved a $\mathrm{TVE}^1_{95}$ below 0.6% at the fundamental, and lower than 4.5% for all the considered harmonics.

In addition, as performance benchmark, the nonlinear inductor has been modeled with a well-known reference method: the complete, third-order, frequency-domain polynomial representation [22]. It has been implemented by following the systematic method presented in [25], that allows writing the structure of frequency-domain Volterra models of arbitrary order excited by periodic multisine inputs.

The identification procedure has been carried out as for the simplified models, and the $\mathrm{TVE}^1_{95}(m)$ values have been computed. It should be noticed that the full third-order Volterra model is defined by 248 coefficients, slightly higher than the number of those characterizing the simplified ninth-order model (231). Therefore, it is interesting to compare the accuracy of the complete third order polynomial model not only with the simplified one having the same order of nonlinearity (counting only 38 coefficients), but also with the ninth order which has a similar complexity. Results are reported in Fig. 5 and TABLE III.

In spite of the considerably higher number of coefficients, the accuracy of the complete third order model is only marginally better than that of the simplified one. On the contrary, the simplified ninth order model is much more accurate, especially at the low harmonics order. For example, the complete third order model achieves a $\mathrm{TVE}^1_{95}$ equal to 15.1% and 32.3% in predicting the fundamental and third order current harmonics, while the simplified ninth order model results in significantly lower values, namely 0.61% and 1.96% respectively.

Finally, it is interesting to compare the actual current waveform with that predicted by using the proposed approach. A new set of periodic input voltages has been generated for this purpose; each signal consists of a 50 Hz fundamental component with a random amplitude between 80% and 120% of the rated value (uniform probability density function), dc and harmonics (up to the $7^{\text{th}}$) whose magnitudes are obtained from a uniform probability density function ranging between 1% and 5% of the fundamental component, and random phases in the interval $[-\pi, \pi]$. The same voltage signals have been applied to the actual system and to the polynomial models; their outputs have been compared in the time-domain. For each signal, the discrepancy between the predicted and the actual current waveforms can be evaluated computing the Normalized Root Mean Square Error (NRMSE):

$$\mathrm{NRMSE} = \sqrt{\frac{\sum_{n=0}^{N_s} \left(i_L\left(nT_s\right) - i_L^{act}\left(nT_s\right)\right)^2}{\sum_{n=0}^{N_s} \left(i_L^{act}\left(nT_s\right)\right)^2}} \tag{36}$$

where $T_s$ is the sampling time and $N_s$ the number of samples per period. The average value of the NRMSE ($\mathrm{NRMSE}_m$) achieved by each simplified polynomial model is reported

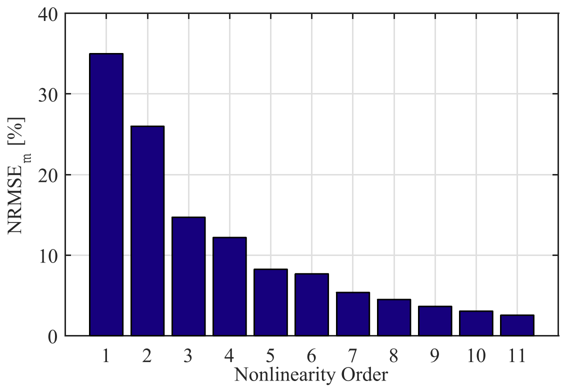


Fig. 6. Comparison between the average NRMSEs achieved by the simplified Volterra models of the nonlinear inductor.

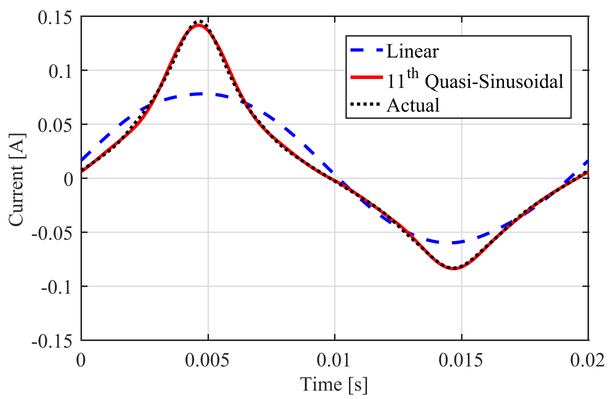


Fig. 7. Predicted current waveforms: linear and eleventh order simplified polynomial model.

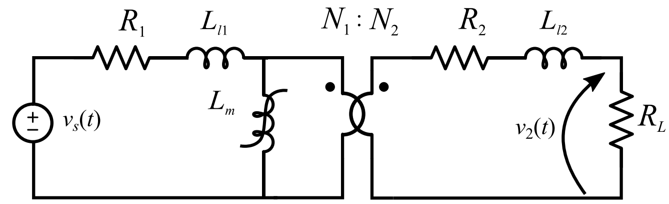


Fig. 8. Equivalent circuit of the voltage transformer.

TABLE IV
VOLTAGE TRANSFORMER SIMULATION PARAMETERS

| $V_{n1}$ [V] | $N_1$:$N_2$ | $R_1$ [Ω] | $R_2$ [Ω] | $L_{l1}$ [mH] | $L_{l2}$ [mH] | $R_L$ [Ω] |
|---|---|---|---|---|---|---|
| 200 | 2 | 6 | 1.25 | 4.75 | 1.19 | 1600 |

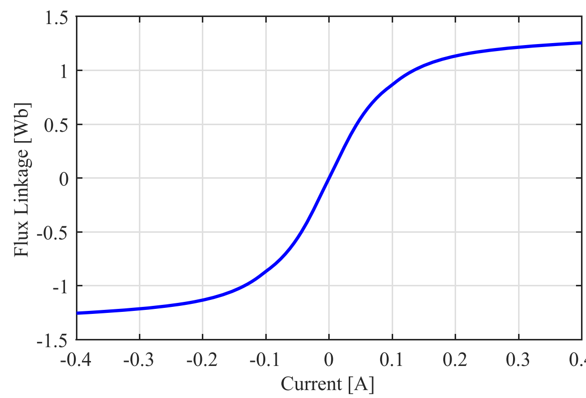


Fig. 9. Flux linkage-current characteristics of the magnetizing inductance.

in Fig. 6. As expected, when the linear model is considered, NRMSE$_m$ is fairly high, being equal to 35%, while increasing the nonlinearity order up to the eleventh it is reduced below 2.5%, that is more than ten times lower. It should be noticed that the complete third order model results in a NRMSE$_m$ of 13.1 %, marginally lower than that of the simplified third-order model (14.7%). In comparison, the simplified ninth order model having similar complexity achieves a considerably lower NRMSE$_m$ equal to 3.64%. An example of reconstructed current signal is reported in Fig. 7, which shows the remarkable accuracy that can be obtained in predicting the output of a heavily nonlinear system by using the proposed approach.

### *B. Voltage Transformer*

In the previous paragraph, the proposed modeling approach has been applied to predict the output of a strongly nonlinear system such as a saturable inductor. Now the target is to accurately model the behavior of a typical power system component characterized by much weaker nonlinearities, such as the input-output relationship of a voltage transformer (VT).

A VT can be represented by the usual equivalent circuit shown in Fig. 8. $R_1$, $R_2$ and $L_{l1}$, $L_{l2}$ represent the winding resistances and leakage inductances, $L_m$ the nonlinear magnetizing inductance, $N_1$:$N_2$ the turn ratio and $R_L$ the burden resistance. The values of the parameters, listed in TABLE IV, refer to an actual class 0.5 VT having 50 Hz rated frequency, 200 V rated primary voltage and 20 VA rated burden. The magnetizing inductance, which is the reason for the nonlinear behavior, is characterized by the single-valued flux linkage-current curve depicted in Fig. 9.

The input voltage is supposed to be periodic, with a main 50 Hz fundamental component and harmonics up to the nineteenth order. Simplified frequency-domain Volterra models having different orders of nonlinearity (from 1 to 11) and a conventional third-order Volterra model have been employed to represent the relationship between the spectrum of the primary voltage $v_s$ (input) and that of the secondary voltage $v_2$ (output). Also in this case, model identification has been performed by using (34) and considering, for each order of nonlinearity, a set of 30 $L$ quasi sinusoidal excitations. These signals contain a fundamental 50 Hz component having random amplitude between 80% and 120% of the rated primary voltage with uniform probability density function. All the harmonics, from the second to the nineteenth have the same amplitude (2% of the fundamental) and random phases, obtained from a uniform probability density function in the range $[-\pi, \pi]$.

For each identification signal, model and harmonic order $m$, the total vector error has been evaluated as indicator of the

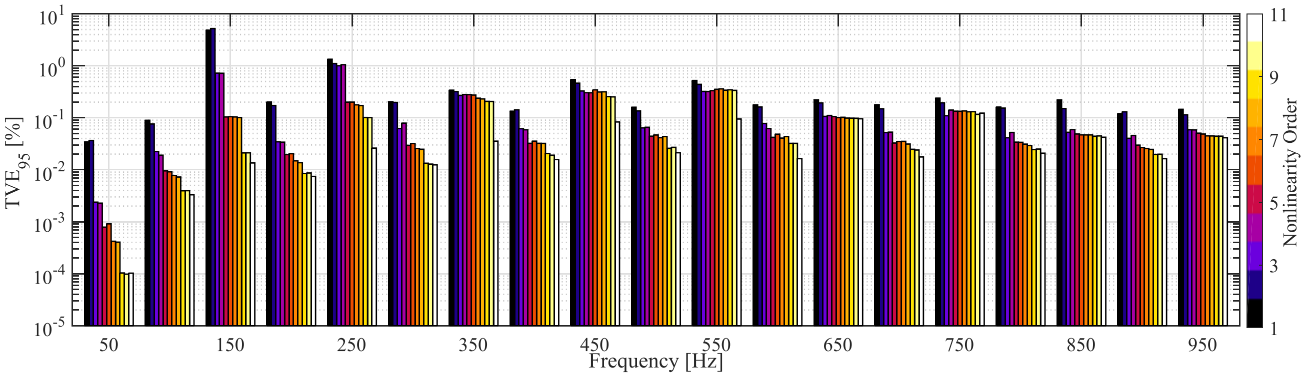


Fig. 10. Accuracy comparison between simplified polynomial models of the voltage transformer.

TABLE V

VOLTAGE TRANSFORMER TVE$_{95}$

| **TVE$_{95}$ [%]** | **Harmonic Order** | | | | | | | | | | | | | | | | | | |
|---|---|---|---|---|---|---|---|---|---|---|---|---|---|---|---|---|---|---|---|
| | **1** | **2** | **3** | **4** | **5** | **6** | **7** | **8** | **9** | **10** | **11** | **12** | **13** | **14** | **15** | **16** | **17** | **18** | **19** |
| **Linear** | $3.4\cdot10^{-2}$ | $8.9\cdot10^{-2}$ | 4.9 | $2.0\cdot10^{-1}$ | 1.3 | $2.0\cdot10^{-1}$ | $3.4\cdot10^{-1}$ | $1.3\cdot10^{-1}$ | $5.4\cdot10^{-1}$ | $1.6\cdot10^{-1}$ | $5.2\cdot10^{-1}$ | $1.8\cdot10^{-1}$ | $2.2\cdot10^{-1}$ | $1.8\cdot10^{-1}$ | $2.4\cdot10^{-1}$ | $1.6\cdot10^{-1}$ | $2.2\cdot10^{-1}$ | $1.2\cdot10^{-1}$ | $1.5\cdot10^{-1}$ |
| **3rd QS** | $2.4\cdot10^{-3}$ | $2.2\cdot10^{-2}$ | $7.2\cdot10^{-1}$ | $3.4\cdot10^{-2}$ | 1.0 | $6.2\cdot10^{-2}$ | $2.7\cdot10^{-1}$ | $6.2\cdot10^{-2}$ | $3.3\cdot10^{-1}$ | $6.4\cdot10^{-2}$ | $3.2\cdot10^{-1}$ | $7.8\cdot10^{-2}$ | $1.1\cdot10^{-1}$ | $5.2\cdot10^{-2}$ | $1.1\cdot10^{-1}$ | $4.1\cdot10^{-2}$ | $5.2\cdot10^{-2}$ | $4.0\cdot10^{-2}$ | $5.9\cdot10^{-2}$ |
| **3rd Complete** | $2.2\cdot10^{-3}$ | $1.9\cdot10^{-2}$ | $7.1\cdot10^{-1}$ | $3.2\cdot10^{-2}$ | 1.0 | $6.9\cdot10^{-2}$ | $2.7\cdot10^{-1}$ | $5.4\cdot10^{-2}$ | $2.9\cdot10^{-1}$ | $6.1\cdot10^{-2}$ | $3.2\cdot10^{-1}$ | $5.6\cdot10^{-2}$ | $1.0\cdot10^{-1}$ | $4.8\cdot10^{-2}$ | $1.2\cdot10^{-1}$ | $4.5\cdot10^{-2}$ | $5.2\cdot10^{-2}$ | $3.9\cdot10^{-2}$ | $5.4\cdot10^{-2}$ |
| **11th QS** | $1.0\cdot10^{-4}$ | $3.3\cdot10^{-3}$ | $1.3\cdot10^{-2}$ | $7.4\cdot10^{-3}$ | $2.6\cdot10^{-2}$ | $1.2\cdot10^{-2}$ | $3.5\cdot10^{-2}$ | $1.6\cdot10^{-2}$ | $8.3\cdot10^{-2}$ | $2.1\cdot10^{-2}$ | $9.5\cdot10^{-2}$ | $1.6\cdot10^{-2}$ | $9.6\cdot10^{-2}$ | $1.8\cdot10^{-2}$ | $1.2\cdot10^{-1}$ | $2.1\cdot10^{-2}$ | $4.2\cdot10^{-2}$ | $1.6\cdot10^{-2}$ | $4.1\cdot10^{-2}$ |

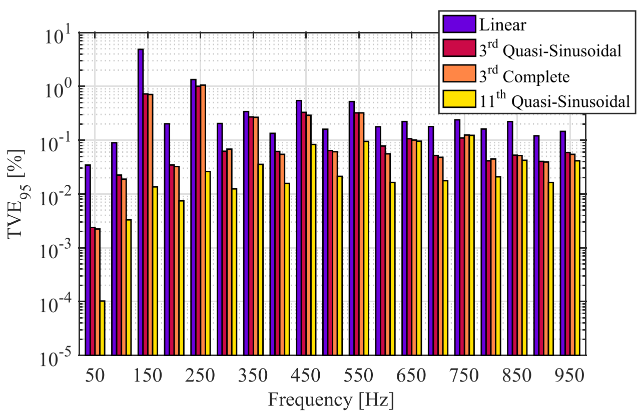


Fig. 11. Comparison between linear, complete third order, simplified third order and simplified eleventh order polynomial models of the voltage transformer.

accuracy. It is defined as:

$$\text{TVE}(m) = \frac{\left|V_2(m) - V_2^{act}(m)\right|}{\left|V_2^{act}(m)\right|} \tag{37}$$

The difference with respect to (35) is that now the error is referred to the amplitude of the $m$-th order output harmonic. The reason is that now the target is to model the impact of the VT nonlinearities on the measurement accuracy of the harmonics. As before, the 95$^{\text{th}}$ percentiles of TVE($m$) have been computed as synthetic indexes of the accuracy; results are reported in Fig. 10, Fig. 11 and summarized in TABLE V. As for the fundamental component, it can be noticed that the voltage transformer nonlinearities have a very small impact, being TVE$_{95}$(1) below 0.04% even when the linear model (frequency response) is employed. Nevertheless, using a simplified polynomial model it can be reduced below $10^{-4}$% (eleventh order model). Nonlinear effects become evident for the other harmonics, especially for the odd ones. The proposed approach is able to take into account these phenomena with excellent accuracy thanks to the spectral content of the input signal. A frequency response-based model achieves a TVE$_{95}$ slightly lower than 5% for the 150 Hz output component; it drops to 0.01% for the eleventh order simplified Volterra model. Also in this case, simulation results show that a complete third order Volterra model results in a accuracy which is just barely better than that achieved by using the simplified approach (Fig. 11 and TABLE V).

It should be noticed that a third order, full polynomial model requires to estimate 3389 coefficients, while this number is reduced to 108 thanks to the quasi-sinusoidal assumption. On the other hand, a simplified eleventh order model is defined by 1074 coefficients and is far more accurate than a complete third-order model having a number of coefficients which is three times higher.

In order to evaluate the performance of the different polynomial models in reconstructing the secondary voltage waveform, the NRMSEs defined in (36) have been evaluated. The comparison between the average NRMSEs obtained by using the simplified models is reported in Fig. 12. As for the TVE, the NRMSE$_m$ values are, in general, very low; however a considerable accuracy improvement can be noticed when the nonlinearity order increases from one (0.04%) to eleven (0.002%). The full third order model achieves an average NRMSE of 0.0111%, five times higher with respect to the simplified eleventh order representation, and just slightly better

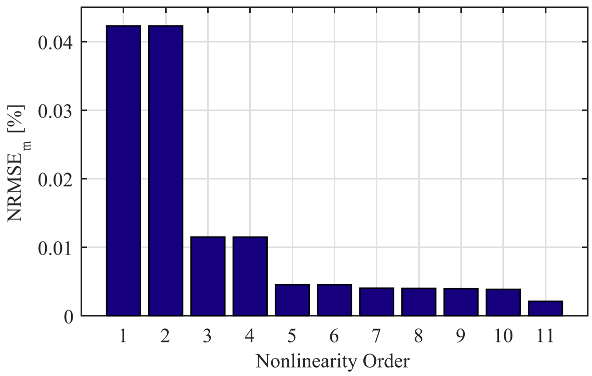


Fig. 12. Comparison between the average NRMSEs achieved by the simplified Volterra models of the voltage transformer.

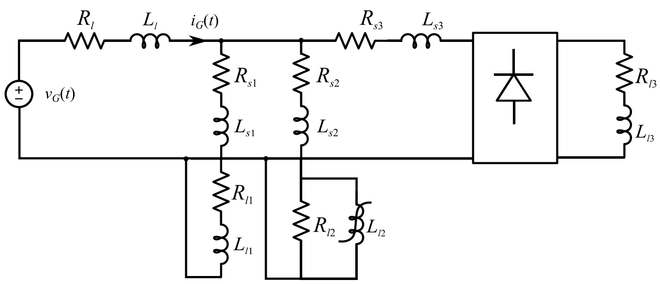


Fig. 13. Equivalent circuit of the grid.

TABLE VI
GRID SIMULATION PARAMETERS

*Line Parameters*

| $R_l$ [Ω] | $L_l$ [mH] | $R_{s1}$ [Ω] | $L_{s1}$ [mH] | $R_{s2}$ [Ω] | $L_{s2}$ [mH] | $R_{s3}$ [Ω] | $L_{s3}$ [mH] |
|---|---|---|---|---|---|---|---|
| 1 | 1 | 10 | 1 | 10 | 1 | 10 | 1 |

*Loads Parameters*

| $R_{l1}$ [Ω] | $L_{l1}$ [mH] | $R_{l2}$ [Ω] | $R_{l3}$ [Ω] | $L_{l3}$ [mH] |
|---|---|---|---|---|
| 7.6 | 0.9 | 1 | 10 | 40 |

than that obtained by using the simplified model having the same nonlinearity order (0.0115 %), albeit the huge difference in complexity.

### *C. Grid With Nonlinear Loads*

In this example, the proposed modeling technique is applied to predict the output current $i_G$ of a distorted ac voltage generator feeding a grid consisting of three different loads: a linear, series *RL* load, a nonlinear inductor (the same described in Section IV-A) and an ideal full-bridge diode rectifier connected to an ohmic-inductive DC load. The equivalent circuit is shown in Fig. 13, while the simulation parameters are listed in TABLE VI.

The voltage $v_G$ is periodic having 50 Hz fundamental frequency and harmonics up to 1 kHz. The magnitude of the fundamental component has been sampled from a uniform probability density function between 80% and 120% of the rated rms voltage $V_n = 230$ V. All the other harmonics have the same amplitude (2% of the fundamental) and random phases, also in this case extracted from a uniform probability density function in the range $[-\pi, \pi]$. A dc component having amplitude equal to 2% of the fundamental and random polarity has been superimposed.

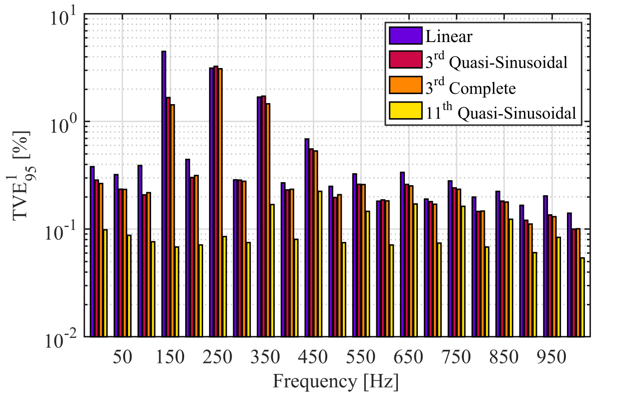


Fig. 14. Comparison between linear, complete third order, simplified third order and simplified eleventh order polynomial models of the grid.

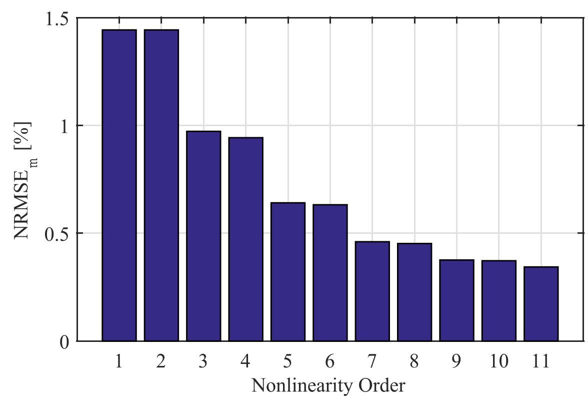


Fig. 15. Comparison between the average NRMSEs achieved by the simplified Volterra models of the grid.

The simplified polynomial models having nonlinearity order from one to eleven have been identified as usual by considering a set of 30 $L$ random excitation signals. As in the previous examples, results have been compared to those obtained with the reference method, namely a full, third order Volterra model identified under the same conditions.

The $\text{TVE}^1$ defined by (35) has been computed for each model, excitation signal and spectral component. Fig. 16 summarizes the $\text{TVE}^1 95^{\text{th}}$ percentile values for the different simplified models.

Nonlinear effects are rather evident in this case study: focusing on the third harmonic component, the linear representation of the system results in a $\text{TVE}^1_{95}$ above 4.5%. The employment of the simplified Volterra model allows a dramatic accuracy improvement in predicting current harmonics, since the error falls below 0.07 % (eleventh order model). These considerations apply similarly for all the other spectral components.

Simulation results show also in this case that the simplified and the full third-order models achieve comparable accuracy,

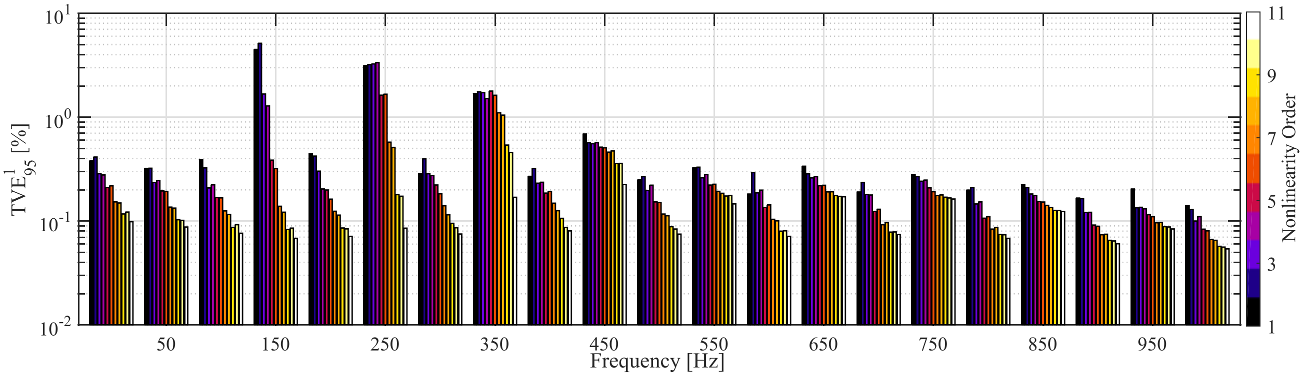


Fig. 16. Accuracy comparison between simplified polynomial models of the grid.

TABLE VII

GRID CURRENT $TVE^1_{95}$

| $TVE^1_{95}$ [%] | Harmonic Order | | | | | | | | | | | | | | | | | | | | |
|---|---|---|---|---|---|---|---|---|---|---|---|---|---|---|---|---|---|---|---|---|---|
| | **0** | **1** | **2** | **3** | **4** | **5** | **6** | **7** | **8** | **9** | **10** | **11** | **12** | **13** | **14** | **15** | **16** | **17** | **18** | **19** | **20** |
| **Linear** | $3.8\cdot10^{-1}$ | $3.2\cdot10^{-1}$ | $3.9\cdot10^{-1}$ | 4.5 | $4.4\cdot10^{-1}$ | 3.1 | $2.9\cdot10^{-1}$ | 1.7 | $2.7\cdot10^{-1}$ | $6.9\cdot10^{-1}$ | $2.5\cdot10^{-1}$ | $3.3\cdot10^{-1}$ | $1.8\cdot10^{-1}$ | $3.4\cdot10^{-1}$ | $1.9\cdot10^{-1}$ | $2.8\cdot10^{-1}$ | $2.0\cdot10^{-1}$ | $2.2\cdot10^{-1}$ | $1.7\cdot10^{-1}$ | $2.0\cdot10^{-1}$ | $1.4\cdot10^{-1}$ |
| **3rd QS** | $2.8\cdot10^{-1}$ | $2.4\cdot10^{-1}$ | $2.1\cdot10^{-1}$ | 1.7 | $3.1\cdot10^{-1}$ | 3.1 | $2.9\cdot10^{-1}$ | 1.7 | $2.3\cdot10^{-1}$ | $5.6\cdot10^{-1}$ | $2.0\cdot10^{-1}$ | $2.6\cdot10^{-1}$ | $1.8\cdot10^{-1}$ | $2.6\cdot10^{-1}$ | $1.8\cdot10^{-1}$ | $2.4\cdot10^{-1}$ | $1.4\cdot10^{-1}$ | $1.8\cdot10^{-1}$ | $1.2\cdot10^{-1}$ | $1.4\cdot10^{-1}$ | $1.0\cdot10^{-1}$ |
| **3rd Complete** | $2.7\cdot10^{-1}$ | $2.3\cdot10^{-1}$ | $2.1\cdot10^{-1}$ | 1.4 | $3.1\cdot10^{-1}$ | 3.1 | $2.8\cdot10^{-1}$ | 1.5 | $2.3\cdot10^{-1}$ | $5.3\cdot10^{-1}$ | $2.0\cdot10^{-1}$ | $2.6\cdot10^{-1}$ | $1.8\cdot10^{-1}$ | $2.5\cdot10^{-1}$ | $1.7\cdot10^{-1}$ | $2.3\cdot10^{-1}$ | $1.4\cdot10^{-1}$ | $1.8\cdot10^{-1}$ | $1.1\cdot10^{-1}$ | $1.3\cdot10^{-1}$ | $1.0\cdot10^{-1}$ |
| **11th QS** | $9.9\cdot10^{-2}$ | $8.8\cdot10^{-2}$ | $7.6\cdot10^{-2}$ | $6.8\cdot10^{-2}$ | $7.1\cdot10^{-2}$ | $8.5\cdot10^{-2}$ | $7.5\cdot10^{-2}$ | $1.7\cdot10^{-1}$ | $8.0\cdot10^{-2}$ | $2.2\cdot10^{-1}$ | $7.5\cdot10^{-2}$ | $1.5\cdot10^{-1}$ | $7.1\cdot10^{-2}$ | $1.7\cdot10^{-1}$ | $7.4\cdot10^{-2}$ | $1.6\cdot10^{-1}$ | $6.8\cdot10^{-2}$ | $1.2\cdot10^{-1}$ | $6.0\cdot10^{-2}$ | $8.4\cdot10^{-2}$ | $5.4\cdot10^{-2}$ |

as reported in Fig. 14 and in TABLE VII, beside the difference in complexity (121 coefficients instead of 4505). On the other hand, a simplified eleventh order model requires estimating 1231 coefficients and results in remarkably better performance.

The overall accuracy of the models is evaluated in terms of NRMSE. For each simplified model the average NRMSE is shown in Fig. 15; its value falls below 0.34% when the eleventh order model is employed. The full and the simplified third order models achieve average NRMSEs of 0.84% and 0.97% respectively.

## V. CONCLUSION

In some applications, such as in ac power systems, nonlinear devices are subject to an input signal containing a strong fundamental component and harmonics that are much smaller in amplitude. This characteristic can be exploited to drastically reduce the number of coefficients of their frequency-domain polynomial models with a negligible impact in terms of accuracy. In this paper, a procedure to define these simplified Volterra models for a generic order of nonlinearity and number of input harmonics has been defined. The algorithm can be easily implemented, and the quasi sinusoidal assumption allows employing high nonlinearity orders which are otherwise unpractical. As case studies, the proposed technique has been employed to represent the input-output relationship of two typical power system devices, showing a very different degree of nonlinearity, and a more complex electrical grid. In all cases, the simplified models achieved remarkable performance. On the one hand, the simplified third order models are almost as accurate as the complete ones beside their considerably lower number of coefficients. On the other hand, the simplified Volterra models allow much better accuracy for the same complexity.

## REFERENCES


[1] R. Pintelon and J. Schoukens, *System Identification: A Frequency Domain Approach*, 2nd ed. New York, NY, USA: Wiley, 2012.

[2] C. Evans and D. Rees, "Nonlinear distortions and multisine signals. I. Measuring the best linear approximation," *IEEE Trans. Instrum. Meas.*, vol. 49, no. 3, pp. 602–609, Jun. 2000.

[3] C. Evans and D. Rees, "Nonlinear distortions and multisine signals. II. Minimizing the distortion," *IEEE Trans. Instrum. Meas.*, vol. 49, no. 3, pp. 610–616, Jun. 2000.

[4] A. F. Esfahani, J. Schoukens, and L. Vanbeylen, "Using the best linear approximation with varying excitation signals for nonlinear system characterization," *IEEE Trans. Instrum. Meas.*, vol. 65, no. 5, pp. 1271–1280, May 2016.

[5] L. Ljung, "Perspectives on system identification," *Annu. Rev. Control*, vol. 34, no. 1, pp. 1–12, 2010.

[6] J. Sjöberg *et al.*, "Nonlinear black-box modeling in system identification: A unified overview," *Automatica*, vol. 31, no. 12, pp. 1691–1724, 1995.

[7] M. Schetzen, *The Volterra and Wiener Theories of Nonlinear Systems*. Hoboken, NJ, USA: Wiley, 2006.

[8] W. J. Rugh, *Nonlinear System Theory: The Volterra/Wiener Approach*. Baltimore, MD, USA: The Johns Hopkins Univ. Press, 1981.

[9] F. Chierchie and S. O. Aase, "Volterra models for digital PWM and their inverses," *IEEE Trans. Circuits Syst. I, Reg. Papers*, vol. 62, no. 10, pp. 2606–2616, Oct. 2015.

[10] A. Stefanou and G. Gielen, "A Volterra series nonlinear model of the sampling distortion in flash ADCs due to substrate noise coupling," *IEEE Trans. Circuits Syst. II, Exp. Briefs*, vol. 58, no. 12, pp. 877–881, Dec. 2011.

[11] H. Yu, K. El-Sankary, and E. I. El-Masry, "Distortion analysis using Volterra series and linearization technique of nano-scale bulk-driven CMOS RF amplifier," *IEEE Trans. Circuits Syst. I, Reg. Papers*, vol. 62, no. 1, pp. 19–28, Jan. 2015.

[12] C. A. Schmidt, J. E. Cousseau, J. L. Figueroa, R. Wichman, and S. Werner, "Non-linearities modelling and post-compensation in continuous-time $\Sigma\Delta$ modulators," *IET Microw., Antennas Propag.*, vol. 5, no. 15, pp. 1796–1804, Dec. 2011.

[13] T. Kamalakis, J. W. Walewski, G. Ntogari, and G. Mileounis, "Empirical Volterra-series modeling of commercial light-emitting diodes," *J. Lightw. Technol.*, vol. 29, no. 14, pp. 2146–2155, Jul. 15, 2011.

[14] V. J. Mathews and G. L. Sicuranza, *Polynomial Signal Processing* (Wiley series in Telecommunications and Signal Processing). New York, NY, USA: Wiley, 2000.

[15] S. A. Billings and S. Y. Fakhouri, "Identification of a class of nonlinear systems using correlation analysis," *Proc. Inst. Electr. Eng.*, vol. 125, no. 7, pp. 691–697, Jul. 1978.

[16] D. Mirri, G. Iuculano, F. Filicori, G. Pasini, G. Vannini, and G. P. Gabriella, "A modified Volterra series approach for nonlinear dynamic systems modeling," *IEEE Trans. Circuits Syst. I, Fundam. Theory Appl.*, vol. 49, no. 8, pp. 1118–1128, Aug. 2002.

[17] C. Crespo-Cadenas, J. Reina-Tosina, M. J. Madero-Ayora, and J. Munoz-Cruzado, "A new approach to pruning Volterra models for power amplifiers," *IEEE Trans. Signal Process.*, vol. 58, no. 4, pp. 2113–2120, Apr. 2010.

[18] A. Zhu and T. J. Brazil, "Behavioral modeling of RF power amplifiers based on pruned Volterra series," *IEEE Microw. Wireless Compon. Lett.*, vol. 14, no. 12, pp. 563–565, Dec. 2004.

[19] M. Li, Z. Yang, Z. Zhang, R. Li, Q. Dong, and S. Nakatake, "Sparsity adaptive estimation of memory polynomial based models for power amplifier behavioral modeling," *IEEE Trans. Microw. Wireless Compon. Lett.*, vol. 26, no. 5, pp. 370–372, May 2016.

[20] A. Zhu, J. C. Pedro, and T. R. Cunha, "Pruning the Volterra series for behavioral modeling of power amplifiers using physical knowledge," *IEEE Trans. Microw. Theory Techn.*, vol. 55, no. 5, pp. 813–821, May 2007.

[21] J. A. Becerra-González, M. J. Madero-Ayora, J. Reina-Tosina, and C. Crespo-Cadenas, "Digital predistortion of power amplifiers using structured compressed-sensing Volterra series," *Electron. Lett.*, vol. 53, no. 2, pp. 89–91, 2017.

[22] L. O. Chua and C.-Y. Ng, "Frequency domain analysis of nonlinear systems: General theory," *IEE J. Electron. Circuits Syst.*, vol. 3, no. 4, pp. 165–185, Jul. 1979.

[23] S. W. Nam and E. J. Powers, "Application of higher order spectral analysis to cubically nonlinear system identification," *IEEE Trans. Signal Process.*, vol. 42, no. 7, pp. 1746–1765, Jul. 1994.

[24] M. Faifer, R. Ottoboni, M. Prioli, and S. Toscani, "Simplified modeling and identification of nonlinear systems under quasi-sinusoidal conditions," *IEEE Trans. Instrum. Meas.*, vol. 65, no. 6, pp. 1508–1515, Jun. 2016.

[25] L. Cristaldi, M. Faifer, C. Laurano, R. Ottoboni, S. Toscani, and M. Zanoni, "Iterative method for the definition of frequency-domain Volterra models," in *Proc. IEEE Int. Instrum. Meas. Technol, Conf.*, May 2017, pp. 1–6.

**Marco Faifer** (S'06–M'10–SM'17) was born in Bormio, Italy, in 1978. He received the M.Sc. degree in electronic engineering and the Ph.D. degree in electrical engineering from the Politecnico di Milano, Milan, Italy, in 2003 and 2009, respectively. He is currently Associate Professor with the Dipartimento di Elettronica, Informazione e Bioingegneria, Politecnico di Milano. His scientific activity is mainly concerned with DSP techniques and the development of industrial sensors and devices for high-voltage measurements. He develops measurement algorithms for the characterization of electrical components and materials. He involves in the field of diagnosis for electrical devices.

**Christian Laurano** (S'16) was born in Lodi, Italy, in 1990. He received the M.Sc. degree in electrical engineering from the Politecnico di Milano, Milan, Italy, where he is currently pursuing the Ph.D. degree in electrical engineering. His research activity is mainly focused on the development of diagnostic techniques for electrical equipment and innovative methods for the characterization of electrical devices and components.

**Roberto Ottoboni** (M'90–F'06) was born in Milano, Italy, in 1961. He received the M.Sc. degree in electronic engineering and the Ph.D. degree in electrical engineering from the Politecnico di Milano in 1988 and 1992, respectively. From 1992 to 1998 and from 1998 to 2002, he was, respectively, an Assistant Professor and an Associate Professor of electrical and electronic measurements, Dipartimento di Elettronica, Informazione e Bioingegneria, Politecnico di Milano, where he is currently a Full Professor of electrical and electronic measurements.

His current research interests are concerned with the application of DSP techniques to electrical measurements and the development of sensors and transducers.

**Marco Prioli** was born in Cesena, Italy, in 1986. He received the M.Sc. and Ph.D. degrees in electrical engineering from the Politecnico di Milano, Milan, Italy, in 2010 and 2014, respectively. From 2014 to 2015, he was a Research Assistant with the Dipartimento di Elettronica, Informazione e Bioingegneria, Politecnico di Milano, where he was involved in the field of electrical measurements and uncertainty evaluation. He is currently involved with the CERN Fellowship Program for the development of the protection of superconducting magnets and circuits of the future circular collider.

**Sergio Toscani** (S'08–M'12) received the M.Sc. *(cum laude)* and Ph.D degrees in electrical engineering from the Politecnico di Milano, Milan, Italy, in 2007 and 2011, respectively. Since 2011, he has been an Assistant Professor in electrical and electronic measurement with the Dipartimento di Elettronica, Informazione e Bioingegneria, Politecnico di Milano.

His research activity is mainly focused on development and testing of current and voltage transducers, measurement techniques for powers systems, electrical components and systems diagnostics.

Dr. Sergio Toscani is member of the IEEE Instrumentation and Measurement Society and the TC-39-Measurements in Power Systems.

**Michele Zanoni** (S'16) was born in Codogno, Italy, 1991. He received the M.Sc. degree *(cum laude)* in electrical engineering from the Politecnico di Milano, Milan, Italy, in 2015, where he is currently pursuing the Ph.D. degree in electrical engineering. His research activity is mainly focused on the development of innovative approaches to the modeling and identification of nonlinear systems devoted to the characterization of current and voltage transducers.